# Structures of viscotoxins A1 and B2 from European mistletoe solved using native data alone

Aritra Pal,[a] Judit É. Debreczeni,[a] Madhumati Sevvana,[a] Tim Gruene,[a] Beatrix Kahle,[b] Axel Zeeck[b] and George M. Sheldrick[a]*

[a]Lehrstuhl für Strukturchemie, Georg-August-Universität, Tammannstrasse 4, D-37077 Göttingen, Germany, and [b]Institut für Organische und Biomolekulare Chemie, Georg-August-Universität, Tammannstrasse 2, D-37077 Göttingen, Germany

Correspondence e-mail: gsheldr@shelx.uni-ac.gwdg.de

Crystals of the cytotoxic thionin proteins viscotoxins A1 and B2 extracted from mistletoe diffracted to high resolution (1.25 and 1.05 Å, respectively) and are excellent candidates for testing crystallographic methods. *Ab initio* direct methods were only successful in solving the viscotoxin B2 structure, which with 861 unique non-H atoms is one of the largest unknown structures without an atom heavier than sulfur to be solved in this way, but sulfur-SAD phasing provided a convincing solution for viscotoxin A1. Both proteins form dimers in the crystal and viscotoxin B2 (net charge +4 per monomer), but not viscotoxin A1 (net charge +6), is coordinated by sulfate or phosphate anions. The viscotoxin A1 crystal has a higher solvent content than the viscotoxin B2 crystal (49% as opposed to 28%) with solvent channels along the crystallographic $4_3$ axes.

## 1. Introduction

The viscotoxins are a group of low-molecular-weight proteins (46 amino acids) found predominantly in the European mistletoe subspecies *Viscum album* Loranthaceae (Romagnoli *et al.*, 2003) that flourishes in the cool damp Göttingen climate. Mistletoe extracts have long been of medical interest (Park, 1881) and have been applied in the treatment of tumours (Friess *et al.*, 1996; Heiny *et al.*, 1998; Steuer-Vogt *et al.*, 2001; Zarkovic *et al.*, 2001). The isolation of viscotoxins from these extracts was reported by Winterfeld (1942) and the term 'viscotoxin' was coined by Winterfeld & Bijl (1948). The viscotoxins all possess a net positively charged surface and contain three conserved disulfide bridges that stabilize their three-dimensional structures (Romagnoli *et al.*, 2000); they also display a high degree of similarity to the plant thionins (Pelegrini & Franco, 2005) and so are classified as type III thionins. To date, seven different viscotoxin isoforms have been reported, namely A1, A2, A3, B, B2, 1-PS and C1, with sequence identities of at least 75% (Fig. 1), in addition to viscotoxin U-PS, which has four disulfides and is more distantly related (Girmann, 2003; Romagnoli *et al.*, 2003; Kahle *et al.*, 2005). The isoform distribution appears to be

```
                        10         20         30         40
                        |          |          |          |
Viscotoxin A1   KSCCPSTTGR NIYNTCRLTG SSRETCAKLS GCKIISASTC PSNYPK
Viscotoxin A2   KSCCPNTTGR NIYNTCRFGG GSRQVCASLS GCKIISASTC PSDYPK
Viscotoxin A3   KSCCPNTTGR NIYNACRLTG APRPTCAKLS GCKIISGSTC PSDYPK
Viscotoxin B    KSCCPNTTGR NIYNTCRLGG GSRERCASLS GCKIISASTC PSDYPK
Viscotoxin B2   KSCCPNTTGR DIYNTCRLGG GSRERCASLS GCKIISASTC PSDYPK
Viscotoxin C1   KSCCPNTTGR NIYNTCRFAG GSRERCAKLS GCKIISASTC PSDYPK
Viscotoxin 1PS  KSCCPNTTGR NIYNTCRFGG GSREVCARIS GCKIISASTC PSDYPK
```

**Figure 1**
Sequence comparison of viscotoxin isoforms.

dependent on the host tree (Schaller *et al.*, 2000). There are appreciable differences in toxicity between the different viscotoxins despite their sequence similarities and the viscotoxins are particularly toxic to tumour cells.

The positively charged surface area common to all the viscotoxins may be involved in interactions with negatively charged molecules such as DNA or phospholipids (Romagnoli *et al.*, 2003; Giudici *et al.*, 2003) and it has long been suspected that several thionins may be involved in phospholipid membrane lysis (Fernandez de Caleya *et al.*, 1972; Carrasco *et al.*, 1981). Stec *et al.* (2004) proposed a detailed model of a thionin–phospholipid complex based on evidence from a variety of experimental methods, although no such complex has yet been crystallized. They proposed that dormant phosphate-bridged thionin dimers split into monomers when they interact with the phospholipid membrane of an invading cell. A hydrophobic patch that had been involved in dimer formation enables the monomer to slide along the hydrocarbon tail of the phospholipid, docking the phosphate head of the phospholipid into the positively charged phosphate-binding site and at the same time interacting with the glyceride branching point. These interactions stiffen the membrane and lead to lysis and permeation of the membrane by, for example, $Ca^{2+}$ ions, which cause further disruption and eventually cell death. A possible interaction between the thionin and the DNA of the cell could take place after rupture of the membrane. The cytotoxic activity of the viscotoxins would be consistent with the observation that eukaryotic tumour cells express a much greater amount of phosphatidylserine in the outer part of the membrane than nontumour cells (Connor *et al.*, 1989).

Crystals of these small relatively rigid sulfur-rich proteins diffract well and are excellent candidates for testing and developing crystallographic methods; the proteins are related to crambin, which in addition to being the first protein structure to be solved by sulfur-SAD (single-wavelength anomalous diffraction) phasing (Hendrickson & Teeter, 1981) has frequently been used successfully as a test structure for *ab initio* direct methods (Sheldrick *et al.*, 2001) and has also been refined against ultrahigh-resolution data (0.54 Å; Jelsch *et al.*, 2000). The crystal structure of viscotoxin A3 was determined by the current authors (Debreczeni, Girmann *et al.*, 2003) by sulfur-SAD phasing. The structures of the A1 and B2 isoforms determined by sulfur-SAD phasing and *ab initio* direct methods, respectively, are reported here. The experience gained in solving these structures will be applicable to other examples in which high-resolution native data are available but only very limited (or even no) initial phase information could be obtained.

## 2. Experimental

### 2.1. Isolation and purification of the viscotoxins

Mistletoe collected from poplar trees was minced and dried at 333 K for 5 d to prevent enzymatic degradation of the target proteins and then ground further to a fine powder. 100 g of this powder was suspended in 2.5 l of 2%(*v/v*) acetic acid pH 4.0 at 277 K for 24 h and sonicated for 30 min using an ultrasound bath. The suspension was filtered and the filtrate was concentrated and passed through a cation-exchange column (SP Sephadex C-25, Sigma–Aldrich; pre-equilibrated with 0.02 *M* ammonium acetate). The column material was rinsed with 700 ml 0.02 *M* ammonium acetate until its colour changed from brown to light fawn. Finally, the material was eluted with 1 *M* ammonium acetate and the eluate was lyophilized. This raw product was dissolved in doubly distilled water and purified by MPLC (medium-pressure liquid chromatography; LiChroprep RP-8, Merck). After loading the sample onto the MPLC column, it was washed first with 450 ml doubly distilled water and then with 450 ml 20%(*v/v*) acetonitrile and 0.1%(*v/v*) trifluoroacetic acid. The mixture of viscotoxins was eluted with 450 ml 40%(*v/v*) aqueous acetonitrile containing 0.1%(*v/v*) trifluoroacetic acid. The isoforms were separated by HPLC (high-performance liquid chromatography; Nucleosil 100 C 8, Jasco; Phenomenex C 18 5μ, Phenomenex) using a water–acetonitrile gradient containing 0.1%(*v/v*) trifluoroacetic acid. Several runs with different gradients were needed to separate all the viscotoxins. 100 g dry mistletoe powder finally yielded 5 mg viscotoxin A1, 8 mg viscotoxin A2, 15 mg viscotoxin A3, 14 mg viscotoxin B, 7 mg viscotoxin 1-PS and 0.2 mg of the newly characterized isoform viscotoxin B2 (Girmann, 2003), which differs from viscotoxin B only in the replacement of Asn11 by Asp.

### 2.2. Crystallization and data collection

All solutions used for crystallization were prepared with doubly distilled water containing 0.03% sodium azide and were sterile-filtered. The lyophilized viscotoxin A1 powder was dissolved in doubly distilled water to obtain a concentration of 15 mg ml$^{-1}$ viscotoxin A1. This solution was centrifuged at 14 000 rev min$^{-1}$ for 2 min to remove insoluble particles. 2 μl of this protein solution was added to 2 μl of a reservoir solution containing 0.1 *M* HEPES [4-(2-hydroxyethyl)-1-piperazine-ethanesulfonic acid] pH 7.5 and 1.4–1.6 *M* trisodium citrate. Crystals appeared after 7 d using the hanging-drop vapour-diffusion method. A crystal of approximate dimensions 0.2 × 0.2 × 0.3 mm was soaked for 30 s in a reservoir solution to which 10%(*v/v*) glycerol had been added as a cryoprotectant and then flash-frozen in a nylon loop. Data were collected at 100 K to a resolution of 1.7 Å on a Bruker M06X rotating-anode generator with Osmic Blue multilayer optics, a three-circle goniometer and a 16 megapixel Smart6000 CCD detector. To ensure a high true redundancy for sulfur-SAD phasing, four 360° $\varphi$-scans with 0.18° oscillation width and nine 180° $\omega$-scans with 0.20° oscillation width were collected. The data-collection strategy was designed to give a uniform high redundancy of about 50 (not merging Friedel opposites) to about 2.2 Å resolution, tailing off to about 5 at the in-house diffraction limit of 1.7 Å. The high redundancy is only required for the data that will be used for phasing. Although these data were truncated for location of the anomalous scatterers, the data to 1.7 Å resolution were

useful for density modification so that interpretable maps could be obtained before taking the crystal off the goniometer. The data collection would have been continued if the maps had not been interpretable. Data were collected, processed, scaled and analyzed using the programs *PROTEUM*, *SAINT*, *SADABS* and *XPREP* (Bruker AXS, 2002). The same crystal was then preserved in liquid nitrogen and subsequently used for synchrotron data collection. For phase extension and final structure refinement, 45 images were collected at an oscillation width of $1°$ to 1.25 Å resolution using a MAR345 detector on beamline BW7B at EMBL/DESY and processed with *HKL*-2000 (Otwinowski & Minor, 1997). Since these data were of good quality and over 99% complete, we did not collect data at different camera distances or merge them with in-house data.

Diffraction-quality crystals of viscotoxin B2 with approximate dimensions of $0.2 \times 0.2 \times 0.5$ mm grew in 2–3 months from droplets containing equal volumes of protein solution (30 mg ml$^{-1}$ in doubly distilled water) and a reservoir solution consisting of 0.20 M (NH$_4$)$_2$SO$_4$, 0.08 M cacodylate buffer pH 6.5 and 35%($v/v$) PEG 8000 or 25% PEG 20 000. The crystals were mounted in nylon loops and soaked for 2–10 min in a cryoprotectant consisting of 75%($v/v$) reservoir solution and 25% glycerol and then flash-cooled in a nitrogen-gas stream at 100 K. The excellent diffraction properties of these crystals allowed data collection in three scans with different detector distances to 1.05 Å resolution on beamline X13 at EMBL/DESY using a wavelength of 0.801 Å and a MAR165 CCD detector. The data were integrated with *HKL*-2000. Data-collection statistics are given in Table 1.

## 2.3. Structure solution of viscotoxin A1 by sulfur-SAD phasing

The ratio $R_{anom}/R_{p.i.m.}$ of 2.60%/0.96% = 2.70 appeared at first sight to be highly favourable for sulfur-SAD phasing {Weiss *et al.*, 2001; $R_{anom} = 200\sum_{hkl} |I(hkl) - \langle I(hkl)\rangle|/\sum_{hkl}[I(hkl) + I(-h-k-l)]$, $R_{p.i.m.} = 100\sum_{hkl}[1(N-1)]^{1/2} \times \sum_i |I_i(hkl) - \langle I(hkl)\rangle|/\sum_{hkl}\sum_i I_i(hkl)$, where $N$ is the number of equivalent reflections in each group of equivalents}. However, this ratio is dominated by the very noisy data at high resolution and thus is misleading; for data to 2.5 Å the corresponding ratio is 1.23%/0.65% = 1.98 and for data in the shell 2.57 to 2.43 Å the ratio is 1.73%/1.22% = 1.42. Nevertheless, these figures are in the range expected for successful sulfur-SAD phasing. The rather low $R_{p.i.m.}$ values play an important role here and confirm the high quality of the merged in-house data.

**Table 1**
Data-collection statistics.

Values in parentheses are for the last resolution shell

|  | Viscotoxin A1 | Viscotoxin A1 | Viscotoxin B2 |
|---|---|---|---|
| X-ray source | Bruker rotating anode | EMBL/DESY BW7B | EMBL/DESY X13 |
| X-ray detector | Bruker Smart6000 CCD | MAR345 image plate | MAR165 CCD |
| Space group | $P4_32_12$ | $P4_32_12$ | $P2_12_12_1$ |
| Unit-cell parameters |  |  |  |
| $a$ (Å) | 65.56 | 65.73 | 39.82 |
| $b$ (Å) | 65.56 | 65.73 | 40.39 |
| $c$ (Å) | 47.08 | 47.16 | 44.69 |
| Wavelength (Å) | 1.5418 | 0.843 | 0.801 |
| Reflections collected | 633456 | 116665 | 680367 |
| Unique reflections | 11828 | 28947 | 34307 |
| Lowest resolution (Å) | 47.2 | 17.0 | 44.7 |
| Highest resolution (Å) | 1.70 (1.79–1.70) | 1.25 (1.35–1.25) | 1.05 (1.15–1.05) |
| Completeness (%) | 100.0 (100.0) | 99.1 (100.0) | 99.8 (99.4) |
| Redundancy | 53.55 (9.71)† | 3.99 (3.96) | 19.79 (17.35) |
| Mean $I/\sigma(I)$ | 43.68 (3.44)† | 15.71 (2.60) | 29.24 (12.83) |
| $R_{int}$‡ (%) | 7.47 (33.36)† | 4.82 (44.49) | 5.72 (18.85) |
| $R_{p.i.m.}$§ (%) | 0.96 (15.53)† | 2.71 (25.09) | 1.53 (4.43) |

† Friedel opposites averaged; when they are not averaged, the redundancy is 29.27 (5.17), the mean $I/\sigma(I)$ is 32.25 (2.86), $R_{int}$ is 7.81 (44.52) and $R_{p.i.m.}$ is 1.28 (21.74), but the completeness is still 100.0 (100.0). ‡ $R_{int} = 100\sum_{hkl}\sum_i |I_i(hkl) - \langle I(hkl)\rangle|/\sum_{hkl}\sum_i I_i(hkl)$. § $R_{p.i.m.} = 100\sum_{hkl}[1/(N-1)]^{1/2}\sum_i |I_i(hkl) - \langle I(hkl)\rangle|/\sum_{hkl}\sum_i I_i(hkl)$, where $N$ is the number of equivalent reflections in each group of equivalents.

A critical decision in weak SAD phasing is the resolution to which the anomalous data should be truncated (Debreczeni, Bunkóczi, Girmann *et al.*, 2003; Debreczeni, Bunkóczi, Ma *et al.*, 2003). One criterion is to truncate at the resolution at which the mean value of $|F_{hkl} - F_{-h-k-l}|/\sigma(F_{hkl} - F_{-h-k-l})$ shown in Fig. 2(a) exceeds about 1.3; for pure noise a ratio of $(2/\pi)^{1/2} = 0.798$ is expected. For these data, this would suggest truncating at about 2.6 Å. The disadvantage of this approach is that it requires accurate estimates of the standard deviations of the reflection intensities. An alternative that does not make this assumption is to calculate the correlation coefficient between the signed anomalous differences between two independent data collections, *e.g.* two separate crystals (Buehner *et al.*, 1974; Schneider & Sheldrick, 2002). In this case, the $\varphi$- and $\omega$-scan data from the same crystal were treated as independent because they had been processed independently (Fig. 2b). A correlation-coefficient threshold of 30% would again lead to truncation of the data at a resolution of 2.6 Å. The data were truncated at the slightly optimistic choice of 2.5 Å. *SHELXD* was instructed to split the super-S atoms (formed by coalescence of the two S atoms of the disulfides) into two individual atoms as part of the peak-search procedure (Debreczeni, Girmann *et al.*, 2003), which gave four solutions for the sulfur substructure with CC in the range 50–52% and CC$_{weak}$ of 27–29% in 1000 trials (Fig. 2c). The 12 correct S atoms were clear above the highest noise peak (Fig. 2d). An exhaustive retrospective analysis showed that it was not possible to obtain a satisfactory solution without the disulfide-splitting option and that the resolution has to be truncated to a resolution of 2.4 Å or lower to obtain a correct solution. The number of hits increased at lower resolution, although the CC and CC$_{weak}$ values remained in the same range. The peak-height discrimination between the weakest S atom and the highest noise peak was optimal with truncation

to a resolution of 2.5 Å and at a resolution lower than about 2.7 Å the disulfide splitting was not so effective. Phasing and density modification in *SHELXE* (Sheldrick, 2002, 2008) using the 12 correct S atoms gave good enantiomorph discrimination and a high-quality map (Fig. 3a) that could be completely traced in 50 cycles by *wARP* (Perrakis *et al.*, 1999). Fig. 3(b) shows the corresponding anomalous map obtained by Fourier back-transformation using the signed anomalous differences as amplitudes and phases obtained by subtracting 90° from the phases from the density modification (Kraut, 1968). This shows the six disulfides as the only anomalous scatterers. All attempts to solve the viscotoxin A1 structure using the 1.25 Å data by strategies similar to the approach that succeeded for the 1.05 Å viscotoxin B2 data failed.

## 2.4. Structure solution of viscotoxin B2 by *ab initio* direct methods

With 861 unique non-H atoms (including water molecules), viscotoxin B2 offered a challenging target for *ab initio* direct methods. Two different structure-solution strategies were tried. One *SHELXD* run was started to search for all atoms directly. A second search was set up to locate first the S atoms only, selecting only the best possible sulfur-substructure solutions on the basis of the correlation coefficient between

**Table 2**
Model-refinement statistics.

|  | Viscotoxin A1 | Viscotoxin B2 |
|---|---|---|
| Resolution range | 17.00–1.25 | 40.00–1.05 |
| No. of reflections | 29166 | 34317 |
| No. of protein residues | 92 | 92 |
| No. of non-H protein atoms | 672 | 664 |
| No. of water molecules | 133 | 105 |
| $R$ factor/free $R$ factor (%) | 12.5/16.7 | 12.7/17.0 |
| R.m.s. deviations from ideal |  |  |
|   Bond lengths (Å) | 0.013 | 0.020 |
|   Angle distances (Å) | 0.028 | 0.034 |
| Ramachandran plot (%) |  |  |
|   Allowed regions | 98.9 | 100.0 |
|   Generously allowed regions | 1.1 | 0.0 |
|   Disallowed regions | 0.0 | 0.0 |
| Mean $B$ values ($\text{Å}^2$) |  |  |
|   Protein (main chain) | 12.5 | 11.5 |
|   Protein (side chain) | 17.2 | 14.9 |
|   Water molecules | 33.4 | 29.2 |
|   Solvent content (%) | 49.1 | 28.3 |
| PDB code | 3c8p | 2v9b |

$E_{\text{obs}}$ and $E_{\text{calc}}$, and then expanding the structure with stepwise peak-list optimization (Sheldrick *et al.*, 2001). The first *SHELXD* run did not give any solutions within a week. The second led to a clear solution (with a final CC of 78.3%) in 2.5 d on a 2 GHz single-CPU Xeon machine. For comparison
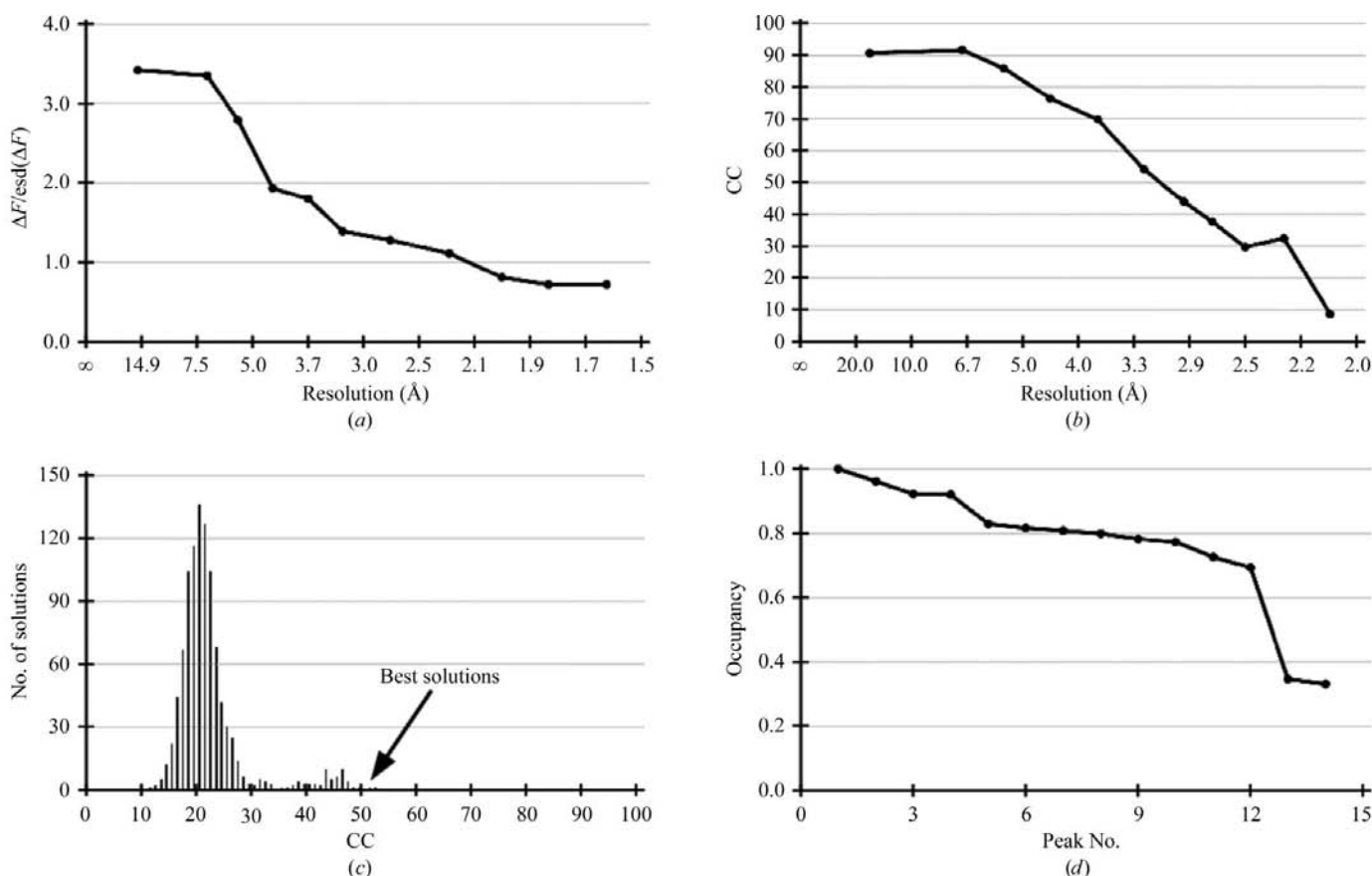


**Figure 2**
Sulfur-SAD phasing statistics for viscotoxin A1: (a) mean $[|F_+ - F_-|/\sigma(F_+ - F_-)]$ against resolution, (b) correlation coefficient between the signed anomalous differences in the $\varphi$ and $\omega$ scans against resolution, (c) histogram of number of solutions in 1000 trials against CC and (d) occupancy against peak number. The figures were drawn with *HKL2MAP* (Pape & Schneider, 2004).

with the peak-list optimization, density modification with *SHELXE* was applied starting from the S atoms located by *SHELXD*; this is similar to the way in which the program *ACORN* can be used to solve structures starting from a few heavier atoms such as sulfur (Yao *et al.*, 2006). This resulted in a very clear high-quality map shown in Fig. 3(*c*) that was used as input for automatic model building with the *wARP* program (Perrakis *et al.*, 1999). After 100 cycles, *wARP* had built the complete model except for four terminal residues, which were added manually.

## 2.5. Structure refinement

Both structures were refined against all $F^2$ data using *SHELXL* (Sheldrick & Schneider, 1997; Sheldrick, 2008),

retaining 5% of the data for calculating the free $R$ factors. Angle-distance, bond-distance, chiral volume and planarity restraints were applied and a Babinet solvent model was employed (Moews & Kretsinger, 1975). All non-H atoms were refined anisotropically with appropriate similar $U_{ij}$, rigid-bond and (for the water molecules) approximately isotropic restraints for the anisotropic displacement parameters; H atoms were included using a riding model. Whereas in the viscotoxin A1 structure only one side chain had to be modelled in an alternative conformation, in viscotoxin B2 there were 13 side chains in alternative conformations. For the A1 structure all the residual electron density around the putative binding site could be modelled as water molecules; in the B2 structure there are five tetrahedral anions that could be assigned as sulfate or phosphate. Refinement statistics are listed in Table 2.

## 3. Discussion

### 3.1. Comparison of viscotoxin monomer structures

The results of least-squares fits of the $C^\alpha$ positions of the six independent monomers in the viscotoxin A1, A3 and B2 structures is presented in Table 3. The six molecules are very similar, especially the two independent A1 monomers (mean deviation of only 0.20 Å). As can be seen in Table 4, the superposition of these six molecules with the ultrahigh-resolution X-ray structure of the plant thionin crambin (PDB code 1ejg; Jelsch *et al.*, 2000) that has one molecule in the asymmetric unit is almost as good, although crambin is less
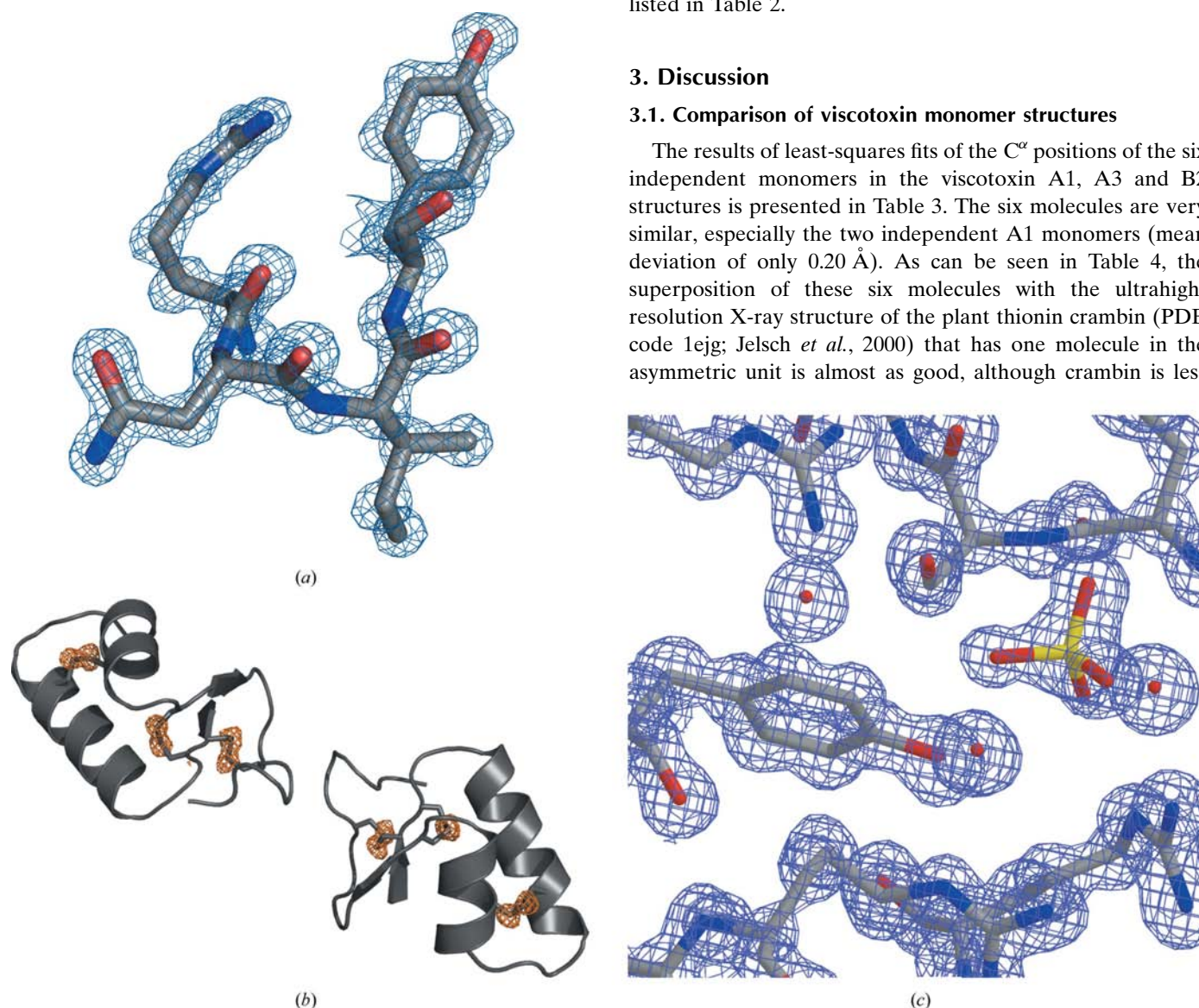


**Figure 3**
(*a*) Experimental density (contoured at 1.5σ) for viscotoxin A1 after density modification of the native 1.25 Å data with *SHELXE* showing residues Arg10, Asn11, Ile12 and Tyr13. (*b*) The corresponding anomalous density (5.0σ) obtained by Fourier back-transformation using the signed observed anomalous differences to 1.70 Å as amplitudes and phases obtained by subtracting 90° from the phases from density modification (Kraut, 1968), showing the disulfides. (*c*) Experimental *SHELXE* density (1.0σ) from the *ab initio* direct-methods solution of viscotoxin B2 calculated using the observed structure factors and phases from direct methods followed by density modification with *SHELXE* using the full 1.05 Å data.

**Table 3**
R.m.s. deviations (Å) between $C^{\alpha}$ atoms after fitting the viscotoxin A1, A3 and B2 molecules found in the crystal structures to one another.

| Molecule | A1 B | A3 A | A3 B | B2 A | B2 B |
|---|---|---|---|---|---|
| A1 A | 0.20 | 0.44 | 0.49 | 0.62 | 0.49 |
| A1 B | | 0.48 | 0.52 | 0.60 | 0.48 |
| A3 A | | | 0.42 | 0.76 | 0.48 |
| A3 B | | | | 0.68 | 0.39 |
| B2 A | | | | | 0.62 |

**Table 4**
R.m.s. deviations (Å) between $C^{\alpha}$ atoms after fitting the viscotoxin A1, A3 and B2 molecules from the crystal structures against crambin in the crystal (PDB code 1ejg) and the NMR structures of viscotoxins A2 (1jmn), A3 (1ed0), B (1jmp) and C1 (1orl).

| Molecule | Crambin | A2 NMR | A3 NMR | B NMR | C1 NMR |
|---|---|---|---|---|---|
| A1 A | 0.63 | 1.31 | 0.84 | 1.38 | 1.27 |
| A1 B | 0.69 | 1.32 | 0.90 | 1.37 | 1.32 |
| A3 A | 0.59 | 1.43 | 0.86 | 1.31 | 1.16 |
| A3 B | 0.54 | 1.38 | 1.03 | 1.35 | 1.15 |
| B2 A | 0.80 | 1.32 | 0.93 | 1.37 | 1.31 |
| B2 B | 0.63 | 1.27 | 0.94 | 1.37 | 1.18 |

positively charged (its pI is between 5.6 and 6.0 depending on the isoform and on whether it is measured or estimated; the pI values of the viscotoxins are 8.5 or higher) and does not act in the same way as the viscotoxins. The charge–activity relation in thionins has been discussed in detail by Giudici *et al.* (2003) and Pelegrini & Franco (2005). Table 4 also shows the r.m.s. (root-mean-square) deviations of the $C^{\alpha}$ positions from the averaged NMR structures of viscotoxins A2 and B (PDB codes 1jmn and 1jmp; Coulon *et al.*, 2003), A3 (PDB code 1ed0; Romagnoli *et al.*, 2000) and C1 (PDB code 1orl; Romagnoli *et al.*, 2003). Despite the good overall agreement, the larger deviations between the NMR and crystal structures than between the viscotoxin crystal structures themselves almost certainly reflect differences in the two techniques rather than real structural differences between solution and crystal. Although the viscotoxin A1 crystal has a much higher solvent content (49% rather than 28%) and looser packing than B2, the monomer backbone structures are in close agreement. The viscotoxin backbone appears to be rather rigid and is little affected by the differences in sequence or by the molecular environment.

## 3.2. Viscotoxin dimers and their interactions with anions

Fig. 4 shows a comparison of the dimers found in the crystal structures of viscotoxins A1, A3 and B2. In the case of viscotoxin A1, these dimers lie on crystallographic twofold axes and so possess exact twofold rotational symmetry. In the case of viscotoxin A3, the two molecules are related by a rotation of 178° and the angle between this rotation axis and the line joining the two molecular centres is 88°, so the noncrystallographic symmetry (NCS) is close to the exact situation characterized by angles of 180° and 90°. For viscotoxin B2, NCS is only approximately fulfilled, with corresponding angles of 168° and 103°. In viscotoxin B2 the deviation from ideal NCS is required to prevent the residue Arg25 from clashing with its NCS equivalent, as can be seen in Fig. 5(*a*); in the other two structures this residue is a threonine and an exact twofold rotation dimer can be formed without a steric clash. Fig. 5 also shows that the positively charged viscotoxin B2 molecules (the net charge per monomer would be +4 assuming for simplicity that the carboxylates are ionized and that the $-NH_2$ groups and arginines are protonated; there are no histidines) are linked by sulfate anions (used for crystallization) or possibly phosphates (retained during the purification). The 1.05 Å resolution experimentally phased (and hence essentially bias-free) map (Fig. 3*c*) is so clear that

no other interpretation of this density is possible. On the other hand, the viscotoxin A1 crystals, for which citrate rather than sulfate was used for crystallization, showed no electron density that could be interpreted as recognisable anions in the experimentally phased and difference maps or in the anomalous map (Fig. 3*b*), so all the solvent was modelled as water
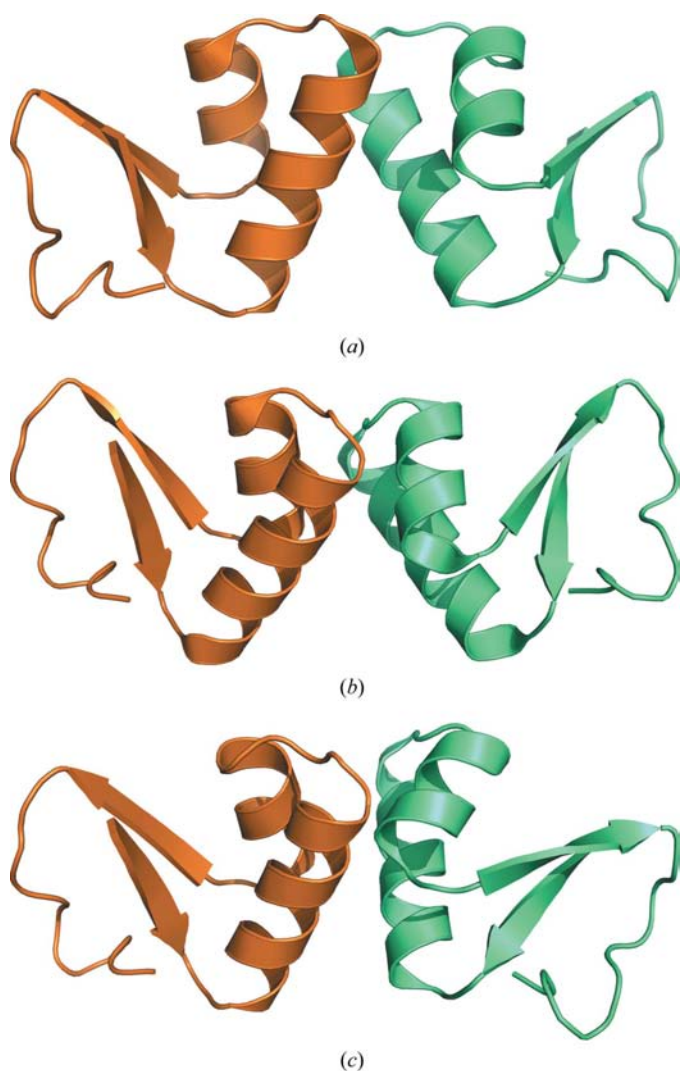


**Figure 4**
Secondary structure and dimer formation in (*a*) viscotoxin A1, (*b*) viscotoxin A3 and (*c*) viscotoxin B2.

molecules despite the net charge of +6 per monomer. The viscotoxin A1 crystal contains helices along the crystallographic $4_3$ axes that enclose solvent channels. It is possible that if as generally assumed the viscotoxin molecules interact with, for example, phosphatidylserine anions, such channels could play a role in the observed lysis of the phospholipid membrane.

## 4. Conclusions

The fact that viscotoxin B2, with native data to a maximum resolution of 1.05 Å, can be solved by *ab initio* direct methods, whereas data to 1.25 Å appear to be insufficient for *ab initio* structure solution of viscotoxin A1, is a further confirmation of the general rule that a resolution of at least 1.2 Å is required for such methods (Sheldrick, 1990; Morris & Bricogne, 2003), although we note that there are indications that combined Patterson and direct methods can be effective at lower resolution, especially when heavier atoms are present (Caliandro

*et al.*, 2007). Viscotoxin A1 is in many respects a favourable case for in-house sulfur-SAD phasing, but even then it was necessary to employ highly redundant data, to take advantage of the presence of disulfide bridges and to choose carefully the resolution at which the data needed to be truncated in order to locate the anomalous scatterers.

Viscotoxins A1, A3 and B2 all form similar dimers in the crystal, although in viscotoxin A1 the dimers involve symmetry equivalents. As proposed by Stec *et al.* (2004), the conserved hydrophobic patches that are protected from solvent by this dimerization could be involved in the binding of the monomers to the hydrophobic part of phospholipids *in vivo*. Whereas the positively charged surface is unambiguously involved in interactions with phosphate or sulfate anions in viscotoxin B2 and probably also in the lower resolution A3 structure (Debreczeni, Girmann *et al.*, 2003), no such anions could be identified in the viscotoxin A1 crystal. This is surprising because anions should be present for electrical neutrality of the crystal, but at 1.25 Å resolution they should be clearly distinguishable from solvent water molecules unless, as seems likely, they are highly disordered.
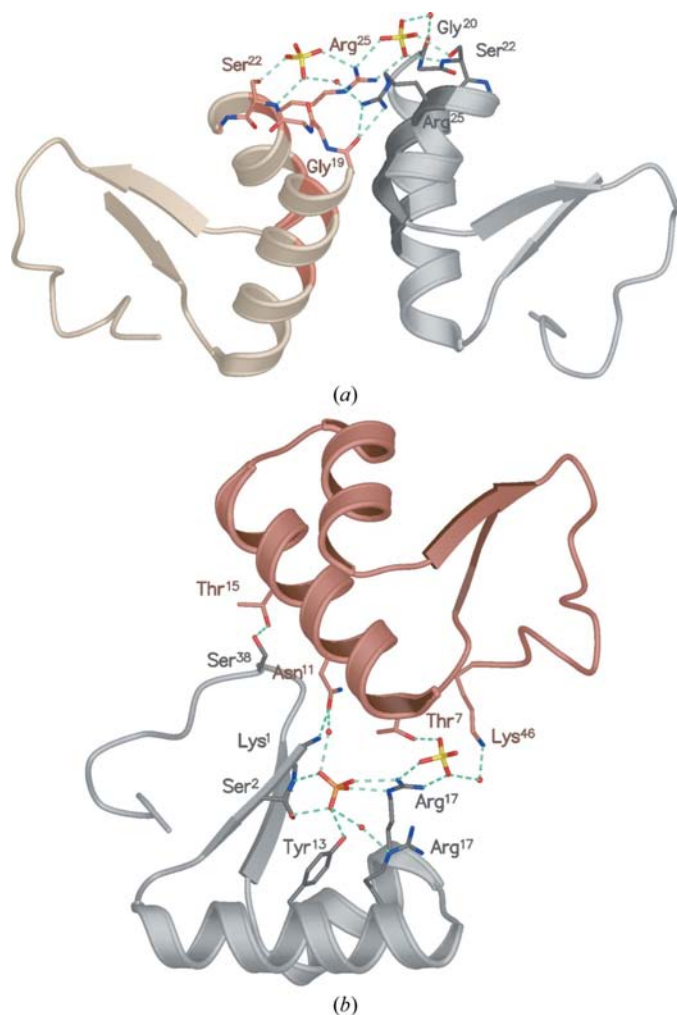
**Figure 5**
Anion- and water-mediated interactions in viscotoxin B2. (*a*) These interactions, particularly those involving Arg25, strengthen the dimers formed by nonpolar interactions but also lead to asymmetry. (*b*) Sulfate- and water-mediated interactions involving a symmetry-equivalent molecule.

## References

Bruker AXS (2002). *PROTEUM, SAINT, SADABS* and *XPREP*. Bruker AXS Inc., Madison, Wisconsin, USA.

Buehner, M., Ford, G. C., Moras, D., Olsen, K. W. & Rossmann, M. G. (1974). *J. Mol. Biol.* **82**, 563–585.

Caliandro, R., Carrozzini, B., Cascarano, G. L., De Caro, L., Giacovazzo, C. & Siliqi, D. (2007). *J. Appl. Cryst.* **40**, 883–890.

Carrasco, L., Vázquez, D., Hernández-Lucas, C., Carbonero, P. & García-Olmedo, F. (1981). *Eur. J. Biochem.* **116**, 185–189.

Connor, J., Bucana, C., Fidler, I. J. & Schroit, A. J. (1989). *Proc. Natl Acad. Sci. USA*, **86**, 3184–3188.

Coulon, A., Mosbah, A., Lopez, A., Sautereau, A.-M., Schaller, G., Urech, K., Rouge, P. & Darbon, H. (2003). *Biochem. J.* **374**, 71–78.

Debreczeni, J. É., Bunkóczi, G., Girmann, B. & Sheldrick, G. M. (2003). *Acta Cryst.* D**59**, 393–395.

Debreczeni, J. É., Bunkóczi, G., Ma, Q., Blaser, H. & Sheldrick, G. M. (2003). *Acta Cryst.* D**59**, 688–696.

Debreczeni, J. É., Girmann, B., Zeeck, A., Krätzner, R. & Sheldrick, G. M. (2003). *Acta Cryst.* D**59**, 2125–2132.

Fernandez de Caleya, R., Gonzalez-Pascual, B., García-Olmedo, F. & Carbonero, P. (1972). *Appl. Microbiol.* **23**, 998–1000.

Friess, H., Beger, H. G., Kunz, J., Funk, N., Schilling, M. & Büchler, M. W. (1996). *Anticancer Res.* **16**, 915–920.

Girmann, B. (2003). PhD thesis, University of Göttingen. Göttingen: Cuvillier Verlag.

Giudici, M., Pascual, R., de la Canal, L., Pfüller, K., Pfüller, U. & Villalain, J. (2003). *Biophys. J.* **85**, 971–981.

Heiny, B. M., Albrecht, V. & Beuth, J. (1998). *Anticancer Res.* **18**, 583–586.

Hendrickson, W. A. & Teeter, M. M. (1981). *Nature (London)*, **290**, 107–113.

Jelsch, C., Teeter, M. M., Lamzin, V., Pichon-Pesme, V., Blessing R. W. & Lecomte, C. (2000). *Proc. Natl. Acad. Sci. USA*, **97**, 3171–3176.

Kahle, B., Debreczeni, J. É., Sheldrick, G. M. & Zeeck, A. (2005). *Fortschritte in der Misteltherapie*, edited by R. Scheer, R. Bauer, H. Becker, V. Fintelmann, F. H. Kemper & H. Schilcher, pp. 83–97. Essen: KVC Verlag.

Kraut, J. (1968). *J. Mol. Biol.* **35**, 511–512.

Moews, P. C. & Kretsinger, R. H. (1975). *J. Mol. Biol.* **91**, 201–228.

Morris, R. J. & Bricogne, G. (2003). *Acta Cryst.* D**59**, 615–617.

Otwinowski, Z. & Minor, W. (1997). *Methods Enzymol.* **276**, 307–326.

Pape, T. & Schneider, T. R. (2004). *J. Appl. Cryst.* **37**, 843–844.

Park (1881). *The Practioner*, **271**, 348.

Pelegrini, P. B. & Franco, O. L. (2005). *Int. J. Biochem. Cell. Biol.* **37**, 2239–2253.

Perrakis, A., Morris, R. J. & Lamzin, V. S. (1999). *Nature Struct. Biol.* **6**, 458–463.

Romagnoli, S., Fogolari, F., Catalano, M., Zetta, L., Schaller, G., Urech, K., Giannattasio, M., Ragona, L. & Molinari, H. (2003). *Biochemistry*, **42**, 12503–12510.

Romagnoli, S., Ugolini, R., Fogolari, F., Schaller, G., Urech, K., Giannattasio, M., Ragona, L. & Molinari, H. (2000). *Biochem. J.* **350**, 569–577.

Schaller, G., Urech, K. & Grazi, G. (2000). *Mistilteinn*, **2000/1**, 32–40.

Schneider, T. R. & Sheldrick, G. M. (2002). *Acta Cryst.* D**58**, 1772–1779.

Sheldrick, G. M. (1990). *Acta Cryst.* A**46**, 467–473.

Sheldrick, G. M. (2002). *Z. Kristallogr.* **217**, 644–650.

Sheldrick, G. M. (2008). *Acta Cryst.* A**64**, 112–122.

Sheldrick, G. M., Hauptman, H. A., Weeks, C. M., Miller, M. & Usón, I. (2001). *International Tables for Crystallography*, Vol. F, edited by E. Arnold & M. Rossmann, pp. 333–351. Dordrecht: Kluwer Academic Publishers.

Sheldrick, G. M. & Schneider, T. R. (1997). *Methods Enzymol.* **277**, 319–343.

Stec, B., Markman, O., Rao, U., Heffron, G., Henderson, S., Vernon, L. P., Brumfeld, V. & Teeter, M. M. (2004). *J. Pept. Res.* **64**, 210–224.

Steuer-Vogt, M. K., Bonkowsky, V., Ambrosch, P., Scholz, M., Neiss, A., Strutz, J., Hennig, M., Lenarz, T. & Arnold, W. (2001). *Eur. J. Cancer*, **37**, 9–11.

Weiss, M. S., Sicker, T. & Hilgenfeld, R. (2001). *Structure*, **9**, 771–777.

Winterfeld, K. (1942). *Pharmaz. Ind.* **9**, 37–41.

Winterfeld, K. & Bijl, L. H. (1948). *Liebigs Ann.* **561**, 107–115.

Yao, J. X., Dodson, E. J., Wilson, K. S. & Woolfson, M. M. (2006). *Acta Cryst.* D**62**, 901–908.

Zarkovic, N., Vukovic, T., Loncaric, I., Miletic, M., Zarkovic, K., Borovic, S., Cipak, A., Sabolovic, S., Konitzer, M. & Mang, S. (2001). *Cancer Biother. Radiopharm.* **16**, 55–62.